Journal of the European Ceramic Society **10** (1992) 299–305

Effect of Powder Processing on Microstructure of Zirconia during Sintering

T. Chartier, T. Gervais

LMCTS (Laboratoire Matériaux Céramiques et Traitements de Surface), URA CNRS 320, ENSCI, 47 à 73 avenue Albert Thomas, 87065 Limoges, France

L. Chermant, J. L. Chermant & M. Coster

LERMAT (Laboratoire d'Etudes et de Recherches sur les Matériaux), URA CNRS 1317, ISMRA, 6 Boulevard du Maréchal-Juin, 14050 Caen, France

(Received 12 November 1991; revised version received 3 February 1992; accepted 28 February 1992)

Abstract

The effect of the processing route on both the sintering and mechanical properties of a stabilized zirconia was investigated.

Zirconia samples prepared by dry pressing and by tape casting are compared from the point of view of microstructural evolution during thermal treatment and from the point of view of mechanical properties. Kinetics of densification and grain growth are studied by automatic image analysis.

The greater homogeneity of the green state obtained by tape casting, in comparison with that obtained by pressing, leads to increased densification and grain growth rates, and to improved mechanical properties.

Es wurde der Einfluß der Herstellungsmethode von stabilisiertem Zirkoniumdioxid auf dessen Sintereigenschaften und dessen mechanische Eigenschaften untersucht.

Die Zirkoniumdioxidproben wurden einerseits durch trockenes Verpressen und andererseits durch Bandgießen hergestellt und hinsichtlich der Gefügeentwicklung bei einer Wärmebehandlung und der mechanischen Eigenschaften untersucht. Die Verdichtungskinetik und das Kornwachstum wurden mittels automatischer Bildanalyse untersucht.

Die bessere Homogenität eines Grünkörpers, der durch Bandguß hergestellt wird, im Vergleich zu einem Grünkörper, der durch Verpressen hergestellt wird, führt zu einer höheren Verdichtungsrate, zu beschleunigtem Kornwachstum und zu verbesserten mechanischen Eigenschaften.

L'influence du procédé expérimental utilisé, sur à la fois les propriétés de frittage et les propriétés mécaniques d'une zircone stabilisée a été étudiée.

Des échantillons de zircone préparés par pressage à sec et par tape casting sont comparés du point de vue de l'évolution microstructurale durant le traitement thermique, et du point de vue des propriétés mécaniques. Les cinétiques de densification et de croissance de grain sont étudiées par analyse automatique d'image.

Une meilleure homogénéité à l'état brut obtenue par tape casting en comparaison avec celle obtenue par compactage conduit à augmenter les taux de densification et de croissance de grain, et à améliorer les propriétés mécaniques.

1 Introduction

The microstructural evolution of ceramic parts during fabrication has to be controlled in order to obtain the required properties (electrical, mechanical, etc.). The two main factors influencing microstructure are powder characteristics and fabrication technique. Powder characteristics are, for example, purity, grain size and shape distributions, specific surface area, quality of the surface and sintering aids. Fabrication includes the processing route and thermal treatments of burning out organic components and sintering. The influence of the microstructure on ZrO_2 mechanical properties has been studied extensively.[1–3] In the ZrO_2–Y_2O_3 system, the ideal microstructure for high strength and high

Journal of the European Ceramic Society 0955-2219/92/$5.00

toughness is the single tetragonal phase with fine and uniform grains.

The aim of this study was to determine the influence of the processing route on the evolution of the microstructure of one TZP powder (ZrO_2 + 3 mol% Y_2O_3) during sintering. Two processing routes were used, dry pressing and tape casting.

2 Experimental

2.1 Starting materials

Zirconia powders stabilized with 3 mol% yttria (Rhône-Poulenc, France) were of two grades: the YZ3 grade with a mean grain size of 0·5 μm and the granulated YZ3 grade with a mean agglomerate size of 56 μm.

Tape casting slurries were composed of YZ3 powder dispersed in a solvent with dispersant, binder and plasticizer additions.[4] The solvent was an azeotropic mixture of 66/34 vol.% 2-butanone/ethanol. The dispersant was a phosphate ester.[5] The binder was a poly(vinyl butyral). The plasticizer was a mixture of poly(ethylene glycol) and dibutyl phthalate.

2.2 Sample preparation

Green sheets with a thickness of 250 μm were tape cast on glass supports. Disks (30 mm diameter) were punched from tapes, stacked and thermocompressed to produce 4-mm-thick samples. Thermocompression was performed at 100°C under a pressure of 60 MPa. The YZ3 granulates were pressed in a floating die under a pressure of 150 Mpa into 30-mm diameter, 4-mm-thick disks. The pyrolysis of organic components was carried out by heating at a rate of 0·2°C/min up to 550°C with a 6-h plateau. The green density was 56% and 60% of theoretical density for pressed and tape cast samples, respectively.

Pressed and tape cast samples were sintered together in an electric furnace with $MoSi_2$ heating elements, in air. The rate was 50°C/min up to 900°C, then 20°C/min up to the sintering temperature (1400 and 1500°C, respectively), the plateau duration ranging from 5 to 1200 min.

2.3 Characterization

The density of sintered samples was measured by the Archimedes technique in distilled water.

The sintered specimens were polished using diamond pastes down to 0·5 μm grade, and then thermally etched for 5 min in air at a temperature 20°C lower than the sintering temperature. SEM micrographs were made of each etched sample, at several positions.

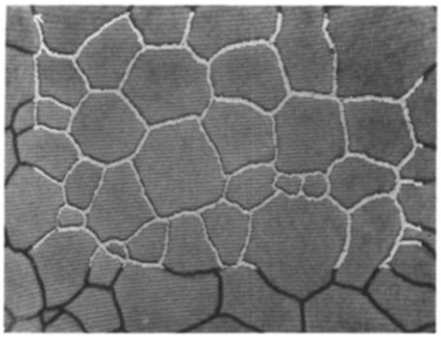

Fig. 1. Binary image obtained by thresholding of the grain boundaries. (11 mm = 0·5 μm.)

The SEM micrographs were analysed using a video camera and an automatic image analyser (NS 1500, Nachet-Microcontrôle, France). Image analysis[6] first means the binarization of SEM micrographs by thresholding (white grain boundaries—level 1, black grains—level 0) (Fig. 1). Then grain boundary thicknesses were reduced to a constant value (1 pixel), using a skeleton by influence zone[6,7] so as not to disturb the stereological analysis (Fig. 2). Two methods can be used to study the granulometric evolution: (i) the measurement of the size of each grain, with the drawback of a great influence of the size of the window, and (ii) granulometric measurement by opening.[7] The latter method is the most suitable in the case of wide granulometric distributions. It is performed by erosion of grains by linear structuring elements of length l. The granulometric density $g(l)$ is calculated using the probability $P(l)$, with the structuring element included in the analysed phase (grains):[6,8]

$$g(l) = lP''(l)/P(0) \qquad (1)$$

$P(l)$ is obtained by measuring the percentage of the eroded phase set by the segment of length l; increasing l values were used until complete removal of grains occurred. $P(0)$ is the percentage of grains; without porosity $P(0)$ is equal to 1. Examples of $P(10)$ and $P(20)$ erosions are shown in Fig. 3.

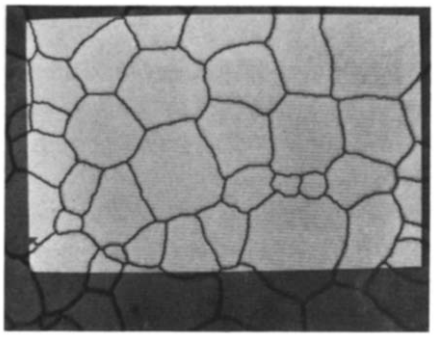

Fig. 2. Final mosaic; the thicknesses of grain boundaries were reduced to 1 pixel. (11 mm = 0·5 μm.)

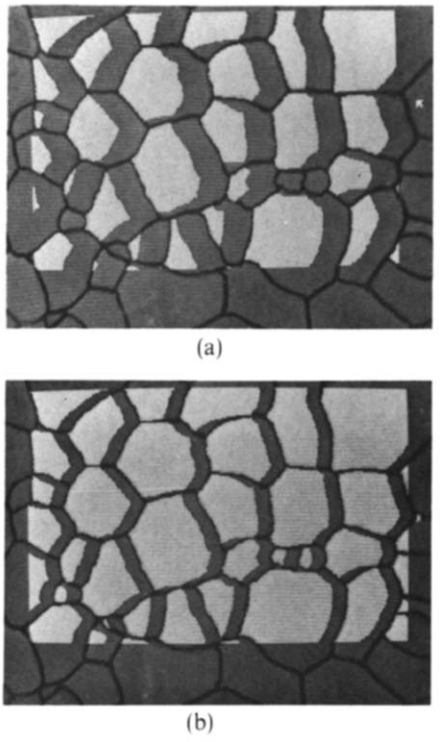

Fig. 3. Erosion by a linear structuring element of (a) 10 and (b) 20 pixels length. (11 mm = 0·5 μm.)

Mean grain sizes G (mean intersected length) were obtained with measurements performed on at least 1000 grains for each processing route and each sintering condition.

Strength was determined, at room temperature, by three-point bending tests at a crosshead speed of 0·5 mm/min. The tensile faces of the samples ($22 \times 4 \times 3\,mm^3$) were polished and the edges were bevelled. Toughness was determined by the single-edge-precracked-beam (SEPB) method,[9] which is an accurate and reliable method. A precrack replaces the notch in the conventional SENB method. Beams similar to those used for strength measurements were polished (0·5 μm). Three Vickers indentations (30 kg, 15 s) as crack starters were made at the centre of the bottom surface. Then beams were precracked on a loading fixture (anvil and pusher); an acoustic device allows the detection of the beginning of the crack extension and unloading to stop the crack propagation. The fracture loads were measured by a three-point bending test and the crack length by optical microscopy. The toughness values were calculated from Strawley's equation.[10]

3 Results and Discussion

Microstructural evolution during thermal treatment can be broadly separated into densification and grain coarsening (grain boundary or surface area reduction at constant density).[11] During sintering,

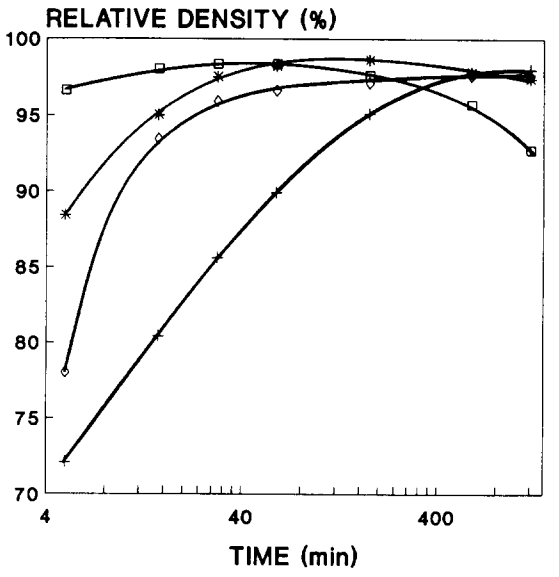

Fig. 4. Relative density versus time for tape cast (◇, □) and pressed (+, ✳) $ZrO_2 + 3\,mol\%\ Y_2O_3$ at 1400°C (◇, +) and 1500°C (□, ✳).

various mechanisms of atom motion may occur. These mechanisms, with the kinetics of densification and grain growth related to grain size evolution, are now well defined.[12]

3.1 Densification

Coble[12] has formulated a diffusion model for the intermediate sintering stage which predicts the densification rate $d\rho/dt$ (for a given temperature and initial microstructure) as a function of the diffusion coefficient responsible for densification ($D_{lattice}$ or $D_{boundary}$) and the average grain size G. The model gives

$$d\rho/dt = CDG^{-n} \qquad (2)$$

where C is a constant. The grain size exponent, n, is 3 and 4, respectively, for densification controlled by lattice-diffusion and grain boundary-diffusion, respectively.

Relative densities versus time are plotted in Fig. 4. The highest densities reached for tape cast and pressed samples were close, i.e. 98·6% of theoretical (6·1 g/cm^3). Densification was faster for tape cast materials than for pressed ones. After 5 min at 1500°C, 96·6% of theoretical density was obtained for tape cast samples, while pressed samples only reached 88·4%. Decreasing density was observed, for 1500°C, after extended sintering times: 60 and 180 min for tape cast and pressed samples, respectively.

3.2 Kinetics of grain growth

The phenomenological kinetic grain growth equation at a temperature T is given by[13]

$$G^m - G_0^m = Kt\exp(-Q/RT) \qquad (3)$$

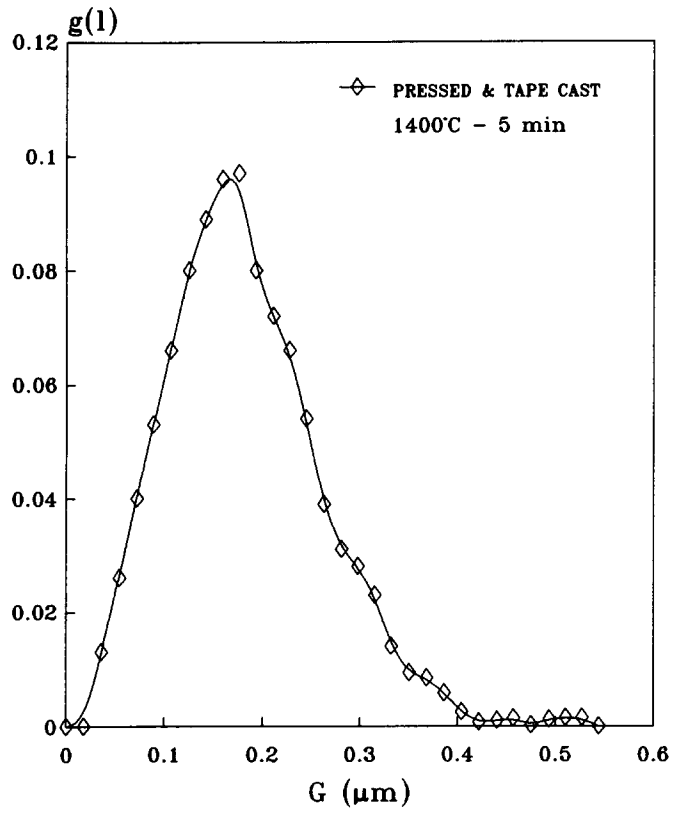

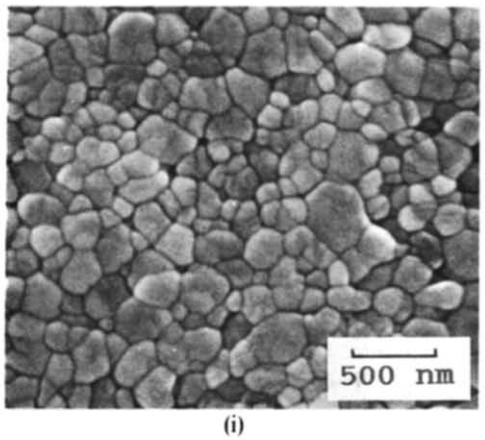

(i)

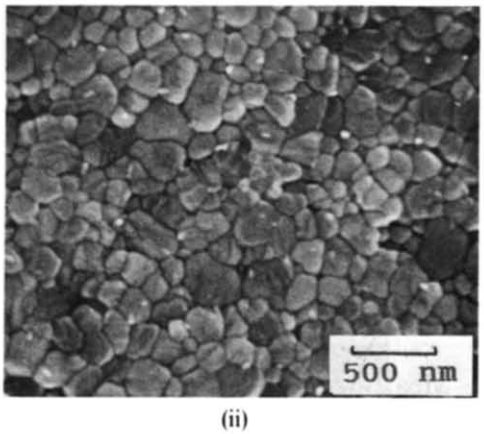

(ii)

(a)

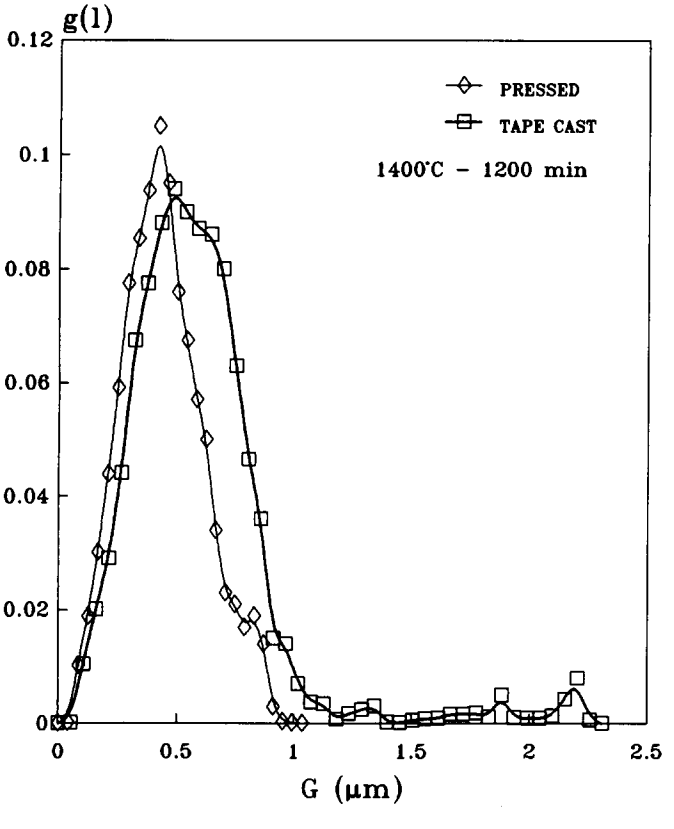

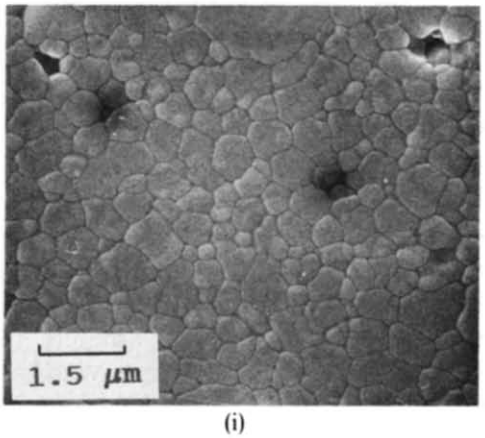

(i)

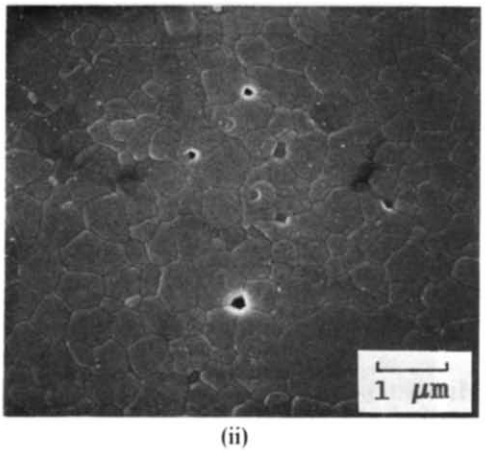

(b) (ii)

Fig. 5. Granulometric densities and corresponding SEM micrographs of (i) tape cast and (ii) pressed ZrO_2 + 3 mol % Y_2O_3 for (a) 5 min and (b) 1200 min at 1400°C, and (c) 600 min at 1500°C.

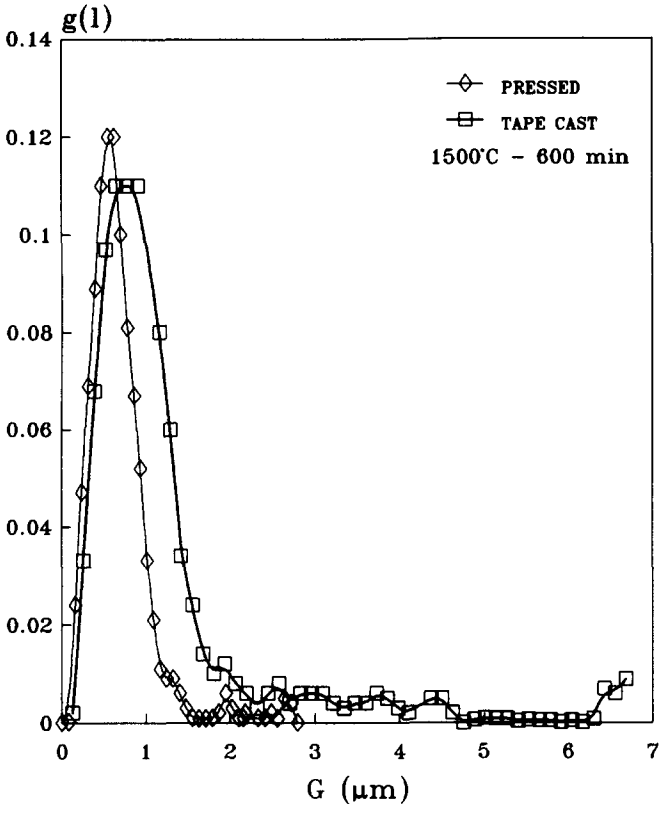

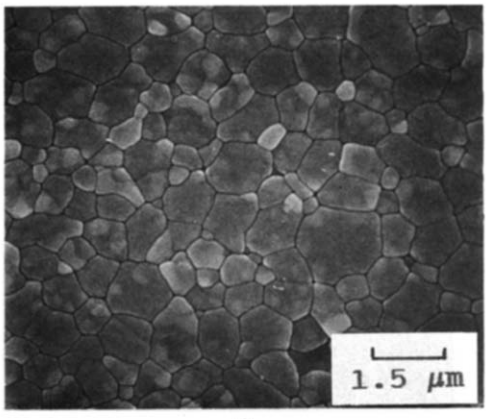

(i)

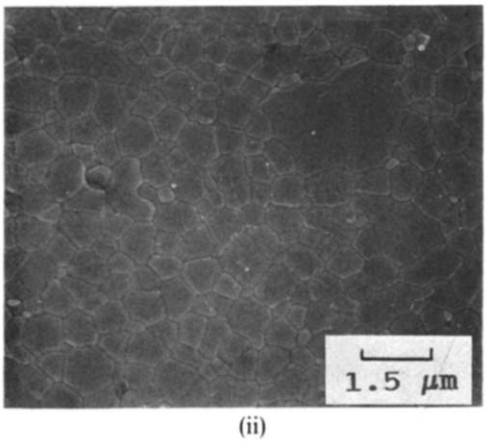

(c) (ii)

Fig. 5.—*Cont.*

where G is the average grain size at time t, G_0 the initial grain size, m the kinetic grain growth exponent, K a constant, Q the apparent activation energy, R the gas constant and T the absolute temperature.

When G becomes significantly greater than G_0 (at longer times), G_0 is generally neglected and the grain growth mechanism can be determined from the slope of the $\ln(G)$ versus $\ln(t)$ line, which is n^{-1}.

Granulometric densities $g(l)$ and corresponding SEM micrographs for tape cast and pressed samples, for 5 and 1200 min at 1400°C and for 600 min at 1500°C, are given in Fig. 5.

Similar granulometric repartitions were found for tape cast and pressed samples sintered for 5 min at 1400°C (0·17 μm). This value is lower than the mean grain size given by the supplier (0·5 μm). This is due to the size distribution methods used, based on different size criteria. The supplier used a sedimentation method based on Stoke's law, while image analysis is based, in that case, on linear measurements on sections. For a same shape of object these values can be correlated. Although results depend on the method used, it does not influence the kinetic grain growth exponent.

Whatever densities and times, larger granulometric distributions were observed with tape cast samples.

The decrease in density can be attributed to release of gas trapped in the material coming from the decomposition of the powder's precursors.[14]

Grain growth versus time is plotted in Fig. 6. The

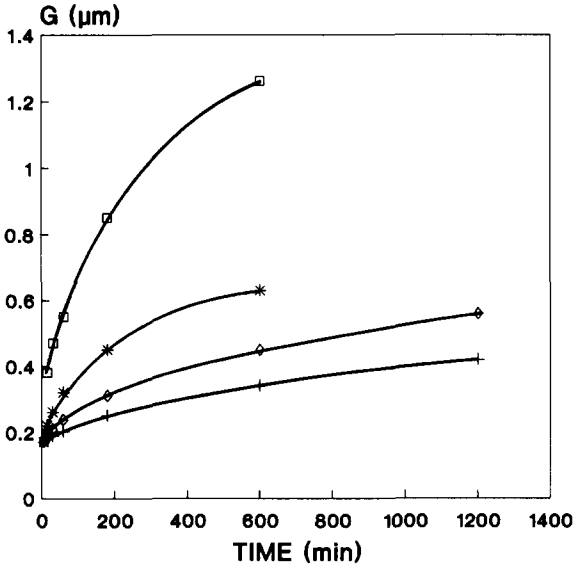

Fig. 6. Mean grain size G versus time for tape cast (◇, □) and pressed (+, ∗) $ZrO_2 + 3\,mol\%\ Y_2O_3$ at 1400°C (◇, +) and 1500°C (□, ∗).

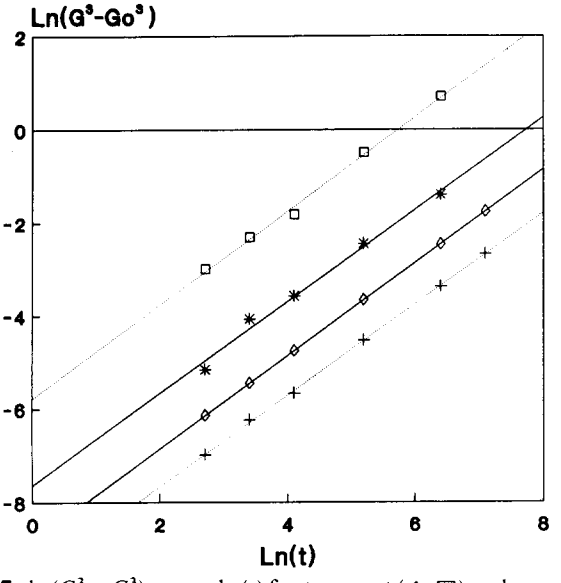

Fig. 7. $\ln(G^3 - G_0^3)$ versus $\ln(t)$ for tape cast (◇, □) and pressed (+, ✳) $ZrO_2 + 3\,mol\%\ Y_2O_3$ at 1400°C (◇, +) and 1500°C (□, ✳) (lines have a slope of 1).

kinetics of grain growth are very slow and the narrow range size (0·17 to 0·56 μm for pressed samples at 1400°C) did not make it possible to neglect the initial grain size G_0 in eqn (3). Correlation coefficients of $\ln(G^m - G_0^m)$ versus $\ln(t)$ are reported in Table 1, with G_0 taken as 0·17 μm. The best correlation was obtained for a kinetic grain growth exponent equal to 3, which is confirmed in Fig. 7. Among possible mechanisms of normal grain growth with a kinetic exponent of 3,[13] the most probable for both tape cast and pressed YZ3 powder, during sintering, was the pore-controlled process with volume diffusion.

Whereas the controlled grain growth mechanism was the same for tape cast and pressed samples, grain growth is faster in tape cast samples. The density and the arrangement of particles in the green state may affect the densification and the grain growth;[15] nevertheless, these parameters are not taken into account by densification and grain growth models. The tape casting process leads to a greater density and homogeneity in the green state.

3.3 Mechanical properties

Strength and toughness results of materials sintered at 1400°C for 10 h are reported in Table 2.

Table 1. Correlation coefficients of $\ln(G^m - G_0^m)$ versus $\ln(t)$ for m equal to 2, 3 and 4

m	1400°C			1500°C		
	2	3	4	2	3	4
Tape cast	0·987	0·999	0·995	0·950	0·999	0·993
Pressed	0·939	0·999	0·987	0·988	0·999	0·994

Table 2. Room-temperature strength (mean value on five samples) and toughness of materials sintered at 1400°C for 10 h

	σ (MPa)	K_{Ic} ($MPa\,m^{1/2}$)	ρ/ρ_{th} (%)	G (μm)
Tape cast	720	7·2	97·6	0·56
Pressed	660	6·5	98·0	0·42

A first comment concerns the strength. Densities and grain sizes are close, but the tape cast material exhibits a higher strength than the pressed one. This confirms that tape casting leads to a very homogeneous green state, with smaller defects.

A second comment concerns the toughness. The toughness of the tape cast material is higher than the pressed one, with a noticeable difference (0·7 MPa $m^{1/2}$) according to the very good reproducibility of K_{Ic} values obtained by the SEPB method.[9] A possible explanation could be related to a beneficial state of residual stresses associated with anisotropic shrinkage. The linear shrinkage along the in-plane direction is higher than in the direction normal to the sheets.

4 Conclusion

This work confirms that the processing route greatly influences the microstructural evolution of ceramic parts during sintering.

Automatic image analysis has proved to be very efficient in characterizing ceramic microstructures.

Tape cast materials exhibit an enhanced densification and grain growth, and improved mechanical properties compared to pressed ones. These results can be related to the very homogeneous green state, with small defects obtained by tape casting.

It was not possible to determine the mechanism of densification because of the large densities obtained above 1400°C and the small increase in grain size. Further work at lower temperature is required to clarify this point. The mechanism of grain growth, i.e. pore drag, is the same in both cases.

References

1. Rühle, M., Claussen, N. & Heuer, A. H., Microstructural studies of Y_2O_3-containing tetragonal ZrO_2 polycrystals (Y-TZP). In *Advances in Ceramics, Vol. 12, Science and Technology of Zirconia*, ed. N. Claussen, M. Rühle & A. H. Heuer. Am. Ceram. Soc., Columbus, OH, 1984, pp. 352.
2. Claussen, N., Microstructural design of zirconia-toughened ceramics (ZTC). In *Advances in Ceramics, Vol. 12, Science and Technology of Zirconia*, ed. N. Claussen, M. Rühle & A. H. Heuer. Am. Ceram. Soc., Columbus, OH, 1984, pp. 325.

3. Tsukuma, K., Kuubota, Y. & Tsukitate, T., Thermal and mechanical properties of Y_2O_3-stabilized tetragonal zirconia polycrystals. In *Advances in Ceramics, Vol. 12, Science and Technology of Zirconia*, ed. N. Claussen, M. Rühle & A. H. Heuer. Am. Ceram. Soc., Columbus, OH, 1984, pp. 382.
4. Boch, P. & Chartier, T., Ceramic processing techniques: the case of tape casting. *Ceram. For. Int.*, **4** (1989) 55.
5. Chartier, T., Streicher, E. & Boch, P., Phosphate esters as dispersants for tape casting of alumina. *Am. Ceram. Soc. Bull.*, **66** (1987) 1653.
6. Coster, M. & Chermant, J. L., Précis d'Analyse d'Images. Editions du CNRS, Paris, France, 1985.
7. Chermant, J. L. & Coster, M., Granulometry and granulomorphy by image analysis. *Acta Stereol.*, **10** (1991) 7.
8. Cerra, J., *Image Analysis and Mathematical Morphology*. Academic Press, New York, 1982.
9. Nose, T. & Fujii, T., Evaluation of fracture toughness for ceramic materials by a single-edge-precracked-beam method. *J. Am. Ceram. Soc.*, **71** (1988) 328–33.
10. Strawley, J. E., Wide range stress intensity factor expressions for ASTM E399 standard fracture toughness specimens. *Int. J. Fract.*, **12** (1976) 475–6.
11. Handwerker, C. A., Cannon, R. M. & Coble, R. L., Final stage sintering of MgO. In *Advances in Ceramics, Vol. 10, Structure and Properties of MgO and Al_2O_3 Ceramics*, ed. W. D. Kingery. Am. Ceram. Soc., Columbus, OH, 1984, pp. 619.
12. Coble, R. L., Sintering crystalline solids. I: Intermediate and final state diffusion models. *J. Appl. Phys.*, **32** (1961) 787–92.
13. Brook, R. J., Controlled grain growth. In *Treatise on Materials Science and Technology, Vol. 9, Ceramic Fabrication Processes*, ed. F. F. Y. Wang. Academic Press, New York, 1976, pp. 331–64.
14. Smith, A. & Baumard, J. F., Sinterability of tetragonal ZrO_2 powders. *Am. Ceram. Soc. Bull.*, **66** (1987) 1144–8.
15. Rahaman, M. N., De Jonghe, L. C. & Chu, M-Y., Effect of green density on densification and creep during sintering. *J. Am. Ceram. Soc.*, **74** (1991) 514–19.